A revised model of Jupiter's inner electron belts: Updating the Divine radiation model

Henry B. Garrett, Steven M. Levin, and Scott J. Bolton
Jet Propulsion Laboratory, California Institute of Technology, Pasadena, California, USA

Robin W. Evans
Gibbel Corporation, Montrose, Pasadena, California, USA

Bidushi Bhattacharya
Spitzer Science Center, California Institute of Technology, Pasadena, California, USA

Received 17 December 2004; revised 3 January 2005; accepted 1 February 2005; published 26 February 2005.

[1] In 1983, Divine presented a comprehensive model of the Jovian charged particle environment that has long served as a reference for missions to Jupiter. However, in situ observations by Galileo and synchrotron observations from Earth indicate the need to update the model in the inner radiation zone. Specifically, a review of the model for 1 MeV < E < 100 MeV trapped electrons suggests that, based on the new synchrotron observations, the pitch angle distributions within L < 4 need to be updated by introducing two additional components: one near the Jovian magnetic equator and one at high magnetic latitudes. We report modifications to the model that reproduce these observations. The new model improves the fit to synchrotron emission observations and remains consistent with the original fit to the in situ Pioneer and Voyager data. Further modifications incorporating observations from the Galileo and Cassini spacecraft will be reported in the future. **Citation:** Garrett, H. B., S. M. Levin, S. J. Bolton, R. W. Evans, and B. Bhattacharya (2005), A revised model of Jupiter's inner electron belts: Updating the Divine radiation model, *Geophys. Res. Lett.*, *32*, L04104, doi:10.1029/2004GL021986.

1. Introduction

[2] *Divine and Garrett* [1983] present a quantitative model of the Jovian charged particle environment that provides a compact means of estimating effects on spacecraft systems in Jupiter's environment and is a standard design reference for missions to Jupiter. Substantial progress in understanding Jupiter's inner radiation belts has been made since the development of the original Divine model (DM). New information from Galileo in situ measurements [*Garrett et al.*, 2003] and ground based radio observations of Jupiter's synchrotron emission [*Bolton et al.*, 2001, 2002] can be used to update the model and provide the basis for improving our understanding of the distribution of high-energy electrons in Jupiter's inner radiation belts and the processes that govern them [*Bolton et al.*, 2004]. Of particular concern is the high-energy electron radiation environment (primarily the 1 to 100 MeV electrons). The new model presented here will assist the investigation of a number of outstanding questions that remain regarding the details of the energy and pitch angle distribution of these electrons trapped in Jupiter's inner belts (reviews of the subject are given by *Bolton et al.* [2004, and references therein]). Here we concentrate on progress in updating the Divine high-energy electron model inside of 4 R_j by matching the spatial distribution to Very Large Array (VLA) maps of Jupiter's synchrotron emission and single-dish beaming curve observations [*Klein et al.*, 1989] (see *Garrett et al.* [2003] for an update between 8–16 R_j).

[3] The new data in the inner region are based on maps of synchrotron radio emissions from Jupiter using the VLA, single-dish observations of the total power versus time and spacecraft observations of Jupiter during the fly-by of Cassini in January 2001 [*Bolton et al.*, 2002]. These data imply that the distribution of particles in the inner region is different than the original DM, with an intense thin "disk" component superimposed on the normal trapped radiation belt component and a set of high latitude lobes [*de Pater et al.*, 1997; *Levin et al.*, 2001]. The DM within 1–4 R_j was originally based on in-situ measurements from Pioneer and early ground-based synchrotron data [*Berge and Gulkis*, 1976; *de Pater and Dames*, 1979] that did not resolve these components. Because of the uncertainties in the older data, it was difficult to reconcile the Pioneer and synchrotron data sources in this inner region—Divine quotes an error of ~10 for the particle intensities inside an L of ~4 [*Divine and Garrett*, 1983]. The new data allow a reassessment of the DM and an opportunity to update the estimates in this uncertain inner region.

[4] Ground-based, single-dish antennas have insufficient spatial resolution to map the inner radiation belts at Jupiter but do accurately measure the systematic variation in total power as Jupiter rotates (the beaming curve). Arrayed antennas can produce interferometric maps of the spatial distribution of emissions near the planet. Synchrotron radiation is highly beamed in the direction of the electron motion with the observed emission depending on the magnetic field strength and direction as well as on the energy and spatial distribution of the electrons. Based on these constraints, an iterative process was used to develop a static model of the radiation belts describing the energy spectrum, radial profile, and pitch angle distributions of the high-energy electrons [*Levin et al.*, 2001]. The sensitivity to errors in the magnetic field model was then tested by producing simulated maps and beaming curves using the

Copyright 2005 by the American Geophysical Union.
0094-8276/05/2004GL021986$05.00

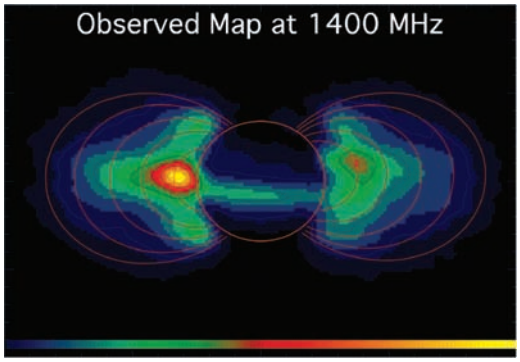

Figure 1a. Observed synchrotron emissions at 1.4 GHz and CML 200° for E > 1 MeV [*Levin et al.*, 2001]. The color scale is linear from 0 (black) to 8.74 × 10^8 Jy/steradian (yellow). Field lines shown correspond to L-shells 1.5, 2.0, 2.5, 3.0, and 3.5 projected onto the meridional plane.

O6 and VIP4 magnetic field models [*Connerney*, 1993; *Connerney et al.*, 1998].

[5] As shown in Figure 1a [*Levin et al.*, 2001], VLA images at decimetric wavelengths indicate the presence of radiating electrons at high magnetic latitudes as well as near the magnetic equator of Jupiter. To reproduce the high latitude emissions, models of the Jovian synchrotron emission usually contain two distinct high-energy electron distributions: a component with small pitch angles and a strongly pancake-shaped component concentrated close to the magnetic equator. Observations of the emissions' polarization and beaming are consistent with this bi-modal electron pitch angle distribution [*Roberts*, 1976].

[6] Levin's static model [*Levin et al.*, 2001] is used here to assess the DM's capability to simulate synchrotron emission observations—the estimated DM synchrotron emission plot is presented in Figure 1b (images are plotted on the same color scale). While differences between the emissions based on the DM and the observations could be due to long term temporal variations, we find that two simple modifications to the DM can account for the majority of differences between them.

2. Changes in the Model

[7] Although the Jovian synchrotron emission levels as viewed from the Earth have varied from ~3.6 Jy to ~5.5 Jy between the 1970s and 1990s [*Bolton et al.*, 2002], evidence suggests that the general emission pattern has been constant. Thus the spatial structure of the original DM needs to be reconsidered. To explore possible modifications, two changes to the DM were introduced, both effective only in the inner magnetosphere. First, the match to the synchrotron observations was improved by slightly reducing the flux for L < 4 and adding a component sharply restricted to pitch angles near 90°. Second, in order to match the observed high-latitude synchrotron lobes, a component is introduced which peaks at low pitch angles within a limited range of L. Each of these changes is discussed below.

[8] *Levin et al.* [2001] showed qualitatively that an isotropic component and an equatorial (pancake) component with pitch angle dependence $\mathrm{Sin}^{40}\alpha$ (where α is pitch angle) matched the synchrotron maps and beaming curves well at 1.4 GHz. To approximate this feature for L < 4, an equatorial component has been added and the original, more isotropic flux reduced by 48% from the original DM. Specifically, we replace the Divine electron flux (F_{DG}) by F_1, with dependence on pitch angle α as shown in equation (1).

$$F_1 = F_{DG}\left(0.48 + 1.80\ \mathrm{Sin}^{40}(\alpha)\right) \tag{1}$$

[9] The observed high-latitude lobes can only be produced by electrons with pitch angles far from the magnetic equator ~90° region. The high latitude lobes are spatially localized, representing electrons with small pitch angles at a narrow range of L-values. To represent this, a component localized between 2.0 < L < 2.3 is added to F_1. This component is most simply approximated by:

$$F_2 = F_1\left(0.6\ \mathrm{Sin}^{-3}(\alpha)\right) \tag{2}$$

For $\alpha > \alpha_c$ where α_c is the critical atmospheric cut-off pitch angle. This component must be feeding the loss cone near L = 2 and requires a process to maintain this distribution since radiation losses, inward radial diffusion and atmospheric losses would deplete this component. The relative importance of these processes is discussed by *Santos-Costa et al.* [2001] and *Bolton et al.* [2004].

[10] The final result, F′, is:

$$\begin{aligned} F' &= F_{DG} \qquad L \geq 4.0 \\ F' &= F_1 + F_2 \quad 2.0 < L < 2.3 \end{aligned} \tag{3}$$

otherwise:

$$F' = F_1 \qquad L \leq 2.0 \text{ or } 2.3 \leq L < 4.0$$

3. Comparison With Observations

[11] In this section, the expected synchrotron emission based on the revised DM is compared with several different

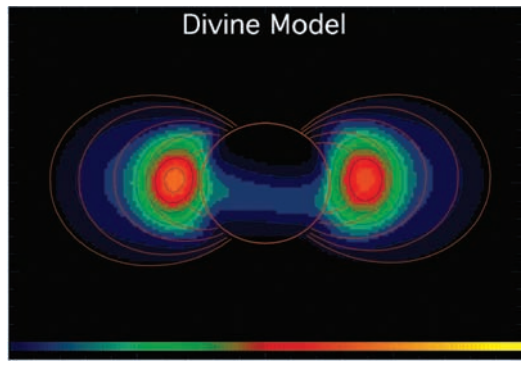

Figure 1b. Predicted 1.4 GHz emissions at CML 200° using the original DM electron radiation distributions for E > 1 MeV. The color scale and field lines are the same in both figures.

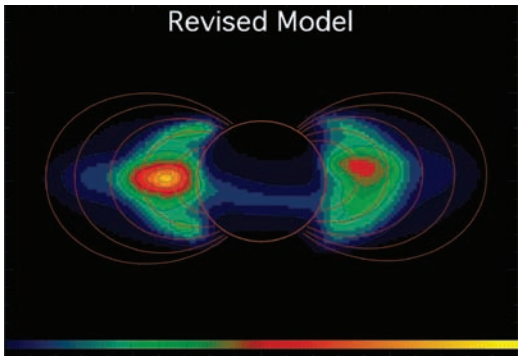

Figure 2. Predicted synchrotron emissions at 1.4 GHz and CML 200° for the modified DM electron radiation distributions for E > 1 MeV. The color scale and field lines are identical to those in Figures 1a and 1b.

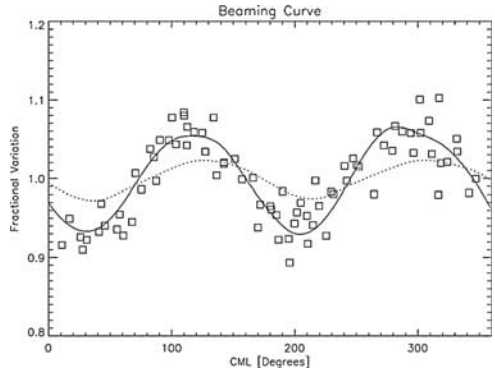

Figure 4. Synchrotron beaming curve at the equator for the modified DM as a function of CML. The dotted line is the original DM, the solid line is the modified version, and the open symbols are the data.

observations. We have not optimized the fit to the synchrotron observations as the data sources and a meaningful quantitative evaluation parameter have yet to be finalized. Rather, we adjusted parameters until agreement between the new model and the different types of observations was judged to be qualitatively adequate. As a first example, Figure 2 illustrates the resulting synchrotron emission image predicted by the modified DM for 1.4 GHz at CML 200° (CML = Central Meridian Longitude). The maps generated from the models have been appropriately averaged over a partial rotation and smoothed to simulate the time averaging and finite spatial resolution associated with the VLA observations. Both components are clearly present and of similar amplitude and location as the observations. Predictions at other CMLs give similar results. In addition to the improved high-latitude lobes, the equatorial emission better matches the asymmetry of the observations—the equatorial electron component combines with the higher order magnetic field terms to produce east-west and north-south asymmetries associated with the shape of the magnetic equatorial surface. Similarly, Figure 3 compares the emission curves for a straight line cut along the magnetic equator at CML = 200° for the synchrotron data, the original DM, and the modified model. The modified Divine model approximates the emission data, duplicating the asymmetry between the east and west portions of the image. Another spatial aspect of the emissions is the equatorial beaming curve. Figure 4 compares this curve as a function of CML for the DM, the new model, and the observations. Agreement between the modified DM and the beaming data is improved over the original DM.

[12] Calculating total synchrotron power as a function of frequency, we find that the modifications introduced here change the frequency spectrum by less than 20%, and remain in rough agreement with observations. The largest discrepancy between model and observations (2.5 more synchrotron emission is predicted by DM than observed by Cassini at 13.8 GHz) is only slightly improved due to these modifications, suggesting the need for optimization of the electron energy distribution.

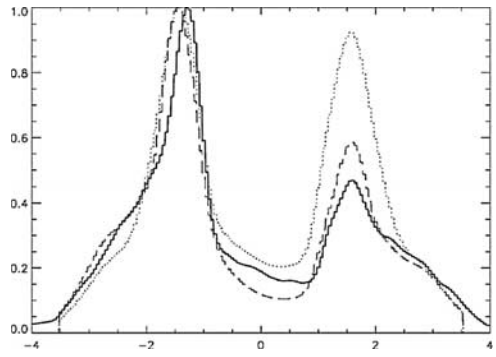

Figure 3. Emission curves for a straight line cut along the magnetic equator at CML = 200° for the synchrotron data (solid line), original DM (dotted), and modified model (dashed). The curves are normalized to a peak value of unity on the vertical (emission) axis. The horizontal axis corresponds to position in R_j along the cut, with Jupiter at the origin. The modified model produces a better match to the observed East-West asymmetry.

4. Comparisons of Revised Model With in Situ Particle Measurements

[13] This section of the paper compares the predicted particle fluences based on the modified DM with the

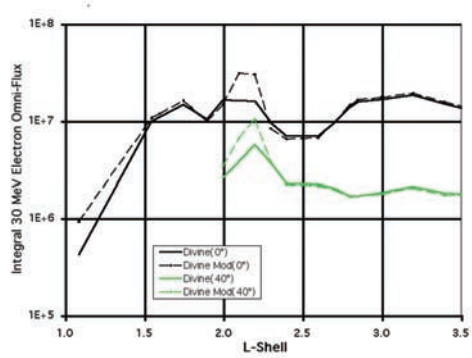

Figure 5. Integral E > 30 MeV electron omni-directional flux along contours at latitudes of 0° and 40° versus L-shell for the original DM (solid lines) and the modified model (dashed lines).

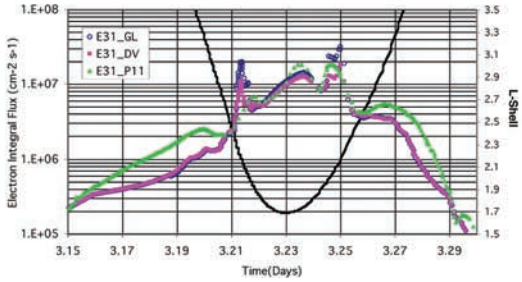

Figure 6. Electron integral fluxes at 31 MeV for the Pioneer 11 fly-by [*Van Allen et al.*, 1975], the original Divine model (DV), and the modified model (GL). Units are particles/(cm^2-s). The black line corresponds to the L-shell for the O6 magnetic field model. The modified model remains consistent with both the Divine model and the Pioneer data over the observed L-shells.

original in situ data. First consider the effect of the changes on the integral omni-directional flux versus L-shell. In Figure 5, the original and modified omni-directional integral electron fluxes are compared at 0° and 40° over a range of L-shells for E = 30 MeV. After integration over pitch angle, the enhancements of the modified model over the original are within a factor of (Modified Flux/Original Flux) < 3.0 with an average value of ~1.25. The primary differences appear at L = 2–2.3 where the high latitude component is important.

[14] Of the Pioneer and Voyager data, the Pioneer 11 orbit demonstrates the largest variation due to the model changes. Figure 6 compares the Pioneer 11 integral flux data at 31 MeV [*Van Allen et al.*, 1975] with the original DM and with the modified version. Note that the new model is within ~3–4 of the Pioneer 11 data—well within the original estimate of a factor of 10.

5. Discussion and Conclusions

[15] The Divine radiation model has been a useful tool for evaluating the Jovian radiation environment for 20 years. Synchrotron observations from the ground suggested that the model inside 4 R_j required updating to incorporate both an equatorial and a high latitude component for E ≥ 1 MeV electrons. In an attempt to update the original model to better represent the synchrotron observations, first order modifications were made to the pitch angle distributions between L-shells of 2 and 4. Although we did not optimize the fits to the observations in a quantitative sense, these simple corrections were found to adequately predict large-scale features in several of the synchrotron observations. This does not represent a unique solution as solutions with slightly different pitch angle distributions could be made to fit equally well, but does indicate the general requirement of a bi-modal electron distribution. Indeed, the electron energy spectrum and its dependence on pitch angle remains an important parameter with insufficient constraints.

[16] *Dulk et al.* [1999a, 1999b] demonstrated the presence of a significant and persistent electron component having equatorial pitch angles $\alpha < 27°$ consistent with the Galileo probe observations of a softer isotropic energy spectrum component and a harder pancake component for L ≤ 2.5 [*Mihalov et al.*, 2000; *Bolton et al.*, 2004]. While comparison of Figures 1a and 2 shows an improvement in the DM capability to reproduce this high latitude emission, the fall off in emission along the field lines toward lower latitudes can be improved with better information on the energy spectrum. Data for this work are in hand and will be analyzed in the future. The source of the increase in small pitch angle electrons at L < 2.3 remains controversial, however, with suggestions ranging from Amalthea to ring effects to natural pitch angle scattering [*Bolton et al.*, 2004]. The sharply defined "pancake" distribution is thought to be a product of adiabatic inward radial diffusion under the influence of satellite sweeping and ring losses [*Bolton et al.*, 1989, 2004]. Finally, the modifications, when integrated over pitch angle, were within a factor of 3 of the original model predictions and within a factor of 3 to 4 of the spacecraft observations in this inner region where Divine quoted an uncertainty factor of ~10. Thus, the fluxes computed for the modified model are within the original model's estimated range relative to the spacecraft and synchrotron data.

[17] **Acknowledgments.** We thank I. Jun and J. M. Ratliff for helpful comments and discussion. This research was carried out at the Jet Propulsion Laboratory, California Institute of Technology, under a contract with the National Aeronautics and Space Administration.

References

Berge, G. L., and S. Gulkis (1976), Earth-based radio observations of Jupiter: Millimeter to meter wavelengths, in *Jupiter*, edited by T. Gehrels, pp. 621–692, Univ. of Ariz. Press, Tucson.

Bolton, S. J., S. Gulkis, M. J. Klein, I. de Pater, and T. J. Thompson (1989), Correlation studies between solar wind parameters and the decimetric radio emission from Jupiter, *J. Geophys. Res.*, *94*, 121–128.

Bolton, S. J., S. M. Levin, S. L. Gulkis, M. J. Klein, R. J. Sault, B. Bhattacharya, R. M. Thorne, G. A. Dulk, and Y. Leblanc (2001), Divine-Garrett model and Jovian synchrotron emission, *Geophys. Res. Lett.*, *28*, 903–906.

Bolton, S. J., et al. (2002), Ultra-relativistic electrons in Jupiter's radiation belts, *Nature*, *415*, 987–991.

Bolton, S. J., R. M. Thorne, S. Bourdarie, I. De Pater, and B. Mauk (2004), Jupiter's inner radiation belts, in *Jupiter: The Planet, Satellites and Magnetosphere*, edited by F. Bagenal, T. Dowling, and W. McKinnon, pp. 671–688, Cambridge Univ. Press.

Connerney, J. E. P. (1993), Magnetic fields of the outer planets, *J. Geophys. Res.*, *98*, 18,659–18,679.

Connerney, J. E. P., M. H. Acuna, N. F. Ness, and T. Satoh (1998), New models of Jupiter's magnetic field constrained by the Io flux tube footprint, *J. Geophys. Res.*, *103*, 11,929–11,939.

de Pater, I., and H. A. C. Dames (1979), Jupiter's radiation belts and atmosphere, *Astron. Astrophys.*, *72*, 148–160.

de Pater, I., M. Schultz, and S. Brecht (1997), Synchrotron evidence for Amalthea's influence on Jupiter's electron radiation belt, *J. Geophys. Res.*, *102*, 22,043–22,064.

Divine, N., and H. B. Garrett (1983), Charged particle distributions in Jupiter's magnetosphere, *J. Geophys. Res.*, *88*, 6889–6903.

Dulk, G. A., Y. Leblanc, R. J. Sault, S. J. Bolton, J. H. Waite, and J. E. P. Connerney (1999a), Jupiter's magnetic field as revealed by the synchrotron radiation belts: I. Comparison of a 3-D reconstruction with models of the field, *Astron. Astrophys.*, *347*, 1029–1038.

Dulk, G. A., Y. Leblanc, R. J. Sault, S. J. Bolton (1999b), Jupiter's magnetic field as revealed by the synchrotron radiation belts: II. Change of the 2-D brightness distribution with DE, *Astron. Astrophys.*, *347*, 1039–1045.

Garrett, H. B., I. Jun, J. M. Ratliff, R. W. Evans, G. A. Clough, and R. W. McEntire (2003), Galileo Interim Radiation Electron Model, *JPL Publ., 03–006*, 85 pp.

Klein, M. J., T. J. Thompson, and S. J. Bolton (1989), Time-variable phenomena in the Jovian system, edited by M. J. S. Belton, *NASA Spec. Publ.*, *SP-494*, 151–155.

Levin, S. M., S. J. Bolton, S. L. Gulkis, M. J. Klein, B. Bhattacharya, and R. M. Thorne (2001), Modeling Jupiter's synchrotron radiation, *Geophys. Res. Lett.*, *28*, 903–906.

Mihalov, J. D., H. M. Fischer, E. Pehlke, and L. J. Lanzerotti (2000), Energetic trapped electron measurements from the Galileo Jupiter probe, *Geophys. Res. Lett.*, *27*, 2445–2448.

Roberts, J. A. (1976), Pitch Angle of electrons in Jupiter's radiation belt, *Proc. Astron. Soc. Aust.*, *3*, 53–55.

Santos-Costa, D., R. Sault, S. Bourdarie, D. Boscher, S. J. Bolton, R. Thorne, Y. Leblanc, G. Dulk, S. M. Levin, and S. Gulkis (2001), Synchrotron emission images from three-dimensional modeling of the electron radiation belts, *Adv. Space Res.*, *28*, 915–918.

Van Allen, J. A., B. A. Randall, D. N. Baker, C. K. Goertz, D. D. Sentman, M. F. Thomsen, and H. R. Flindt (1975), Pioneer 11 observations of energetic particles in the Jovian magnetosphere, *Science*, *188*, 459–462.

B. Bhattacharya, Spitzer Science Center, California Institute of Technology, 1200 E. California, MS 220-6, Pasadena, CA 91125, USA.

S. J. Bolton, H. B. Garrett, and S. M. Levin, Jet Propulsion Laboratory, California Institute of Technology, 4800 Oak Grove Drive, MS 122-107, Pasadena, CA 91109, USA. (henry.garrett@jpl.nasa.gov)

R. W. Evans, Gibbel Corporation, Honolulu Avenue, Montrose, CA 91214, USA.